JOURNAL OF NEUROPHYSIOLOGY
Vol. 75, No. 5, May 1996. *Printed in U.S.A.*

Single-Domain/Bound Calcium Hypothesis of Transmitter Release and Facilitation

RICHARD BERTRAM, ARTHUR SHERMAN, AND ELIS F. STANLEY
Mathematical Research Branch, National Institute of Diabetes and Digestive and Kidney Diseases, National Institutes of Health, Bethesda 20814; and Synaptic Mechanisms Section, National Institute of Neurological Diseases and Stroke, National Institutes of Health, Bethesda, Maryland 20892

SUMMARY AND CONCLUSIONS

1. We describe a model of transmitter release that is based on the finding that release can be gated during the opening of individual Ca^{2+} channels, suggesting that the release site can be activated by the Ca^{2+} domain under a single channel. In this model each release site contains four independent Ca^{2+} binding sites or gates with unbinding kinetics graded from slow to fast and affinities ranging from high to low. All four gates must be bound for release to occur. Thus synaptic dynamics are governed by the kinetics of Ca^{2+} binding and unbinding from release sites, not Ca^{2+} diffusion.

2. Fast facilitation occurs when an action potential invades a terminal with one or more ions remaining bound to the release sites. Residual free Ca^{2+} is not necessary for facilitation with this mechanism, but if present it would enhance facilitation by binding to high-affinity gates between pulses.

3. This model can account for key features of release. These include fourth-power cooperativity with regard to external Ca^{2+}; a release time course that is virtually independent of an increase in quantal content; an inverse relation between external Ca^{2+} and the degree of facilitation; and a steplike increase in facilitation with increasing stimulus frequency, with each step corresponding to a unitary decline in the Ca^{2+} cooperativity.

4. Facilitation of single-channel-based secretion is shown to be robust even if channel opening is stochastic. Spontaneous release of transmitter, assumed to be due in part to spontaneous Ca^{2+} channel openings, is shown to be elevated during and after a train of impulses.

5. An extension of the model to include multiple Ca^{2+} channels per release site demonstrates that one role of overlapping Ca^{2+} domains may be to accentuate depolarization-evoked release relative to spontaneous release.

INTRODUCTION

The seminal work of Katz and Miledi (1968) and Llinás et al. (1981b) on fast synaptic transmission established the importance of Ca^{2+} influx as a critical link between depolarization of the nerve terminal and release of the transmitter substance. Thus it is generally accepted that this ion enters via voltage-sensitive ion channels and then binds to an acceptor to gate quantal transmitter release. Several studies have attempted to describe this mechanism in the form of a mathematical model. These models focused initially only on the kinetics of Ca^{2+} binding to its acceptor. Subsequent models increased in complexity in order to describe other characteristics of transmitter release, notably its time course, its dependence on external Ca^{2+} concentration, and the phenomenon of fast facilitation. In the model of Fogelson and Zucker (1985), both the time course and magnitude of transmitter release were determined by Ca^{2+} diffusion. Problems with this approach were pointed out by Parnas et al. (1989), who favored a model in which the release time course is set by voltage (Parnas et al. 1986a). The Fogelson-Zucker model was later modified to include the kinetics of Ca^{2+} binding to release site acceptors, overcoming some of the criticisms of the pure free-Ca^{2+}-based model (Yamada and Zucker 1992).

Each of these models relies heavily on Ca^{2+} diffusion in setting either the time course or the magnitude of transmitter release. In each case fast facilitation is due primarily to the buildup of free Ca^{2+} at the release site, an idea best termed the residual free calcium hypothesis. We present a model in which the time course of release is determined solely by the binding of Ca^{2+} to acceptors in the release sites. We assume that only Ca^{2+} in the domain immediately adjacent to an open channel is relevant and neglect bulk diffusion of Ca^{2+} between single channels. Facilitation in this case is due to the buildup of Ca^{2+} bound to release sites, an idea proposed previously by Katz and Miledi (1968) and Rahamimoff (1968), rather than to residual free Ca^{2+}. By making the single-domain approximation, we obtain a greatly simplified model that is amenable to mathematical analysis and allows us to explore how much can be explained solely on the basis of Ca^{2+} binding dynamics. We will show that we can reproduce many of the important characteristics of fast transmitter release, and also that the approximation breaks down when prolonged depolarizations are considered, suggesting a role for overlapping domains.

The model presented here is based on the following three properties of synaptic transmission, which we believe are of defining importance in transmitter release.

Experimental basis of the model

DURING ACTION-POTENTIAL-TRIGGERED TRANSMISSION THE RELEASE SITE IS GATED BY Ca^{2+} INFLUX FROM A SINGLE OPEN Ca^{2+} CHANNEL. The observation that the minimal latency between Ca^{2+} influx and transmitter release onset can be as short as 200 μs limits the possible distance from the Ca^{2+} channel to the Ca^{2+} binding sites to within 100 nm (Llinás et al. 1981b). Subsequent studies have concluded that the release site is close enough to the Ca^{2+} channels to be gated by the cloud of Ca^{2+} —a Ca^{2+} domain—that enters during the opening of a single Ca^{2+} channel (Augustine et al. 1991; Stanley 1993; Yoshikami et al. 1989). During an action

potential the relatively slow activation kinetics (Llinás et al. 1981a; Stanley and Goping 1991) of presynaptic Ca^{2+} channels ensure that the distance between simultaneously open channels will, on average, be large. Furthermore, Ca^{2+} influx during an action potential occurs primarily when the membrane potential has repolarized and the driving force for Ca^{2+} entry is great (Llinás et al. 1982). Thus during an action potential the combination of scattered open Ca^{2+} channels and high ion influx per channel favors the activation of release sites by single Ca^{2+} channel domains. Clearly even during action potential-gated transmitter release some release sites will be triggered by Ca^{2+} domains that overlap from neighboring Ca^{2+} channels, but we have assumed that single-domain-based secretion is predominant.

The single-domain assumption is unlikely to be valid when release is gated by prolonged depolarizations, such as during voltage-clamp steps in the squid giant synapse. In such cases the model can be modified to include activation by Ca^{2+} influx from a number of neighboring open channels, generating an overlapping Ca^{2+} domain at the release site.

ACTIVATION OF THE RELEASE SITE REQUIRES THE COOPERATIVE ACTION OF FOUR CALCIUM IONS. It was first noted by Jenkinson (1957) that there is a nonlinear relation between the external Ca^{2+} concentration and the quantity of transmitter released by the nerve impulse. Dodge and Rahamimoff (1967) demonstrated a fourth-power relation, an observation that has been repeatedly observed in a variety of species and over a wide range of Ca^{2+} concentrations. The interpretation of this power dependency was that at least four calcium ions must cooperate to activate the release site. We have assumed that the release site has four Ca^{2+} binding sites, or gates, all of which must be occupied for release to occur.

CALCIUM ACTION AT THE RELEASE SITE DECAYS AT FOUR DIFFERENT DEFINED RATES. The phenomenon of fast facilitation, in which the number of quanta of transmitter released by an impulse is increased if preceded by a conditioning impulse, has been attributed to the continuing activation of the transmitter release sites by Ca^{2+} that entered during the conditioning impulse. An increasing body of evidence (Balnave and Gage 1974; Bittner and Schatz 1981; Blundon et al. 1993; Stanley 1986; Winslow et al. 1994; Younkin 1974) favors facilitation based on residual bound calcium.

A simple mechanism by which residual bound calcium could facilitate transmitter release is to reduce the number of additional calcium ions that need to bind to activate the release site during the next impulse. This mechanism is supported by two observations at the squid giant synapse (Stanley 1986; Liu and Stanley 1995). First, maximum facilitation induced by trains of action potentials increases in a steplike manner as the stimulus frequency is increased, and second, each step corresponds to a unitary decline in the Ca^{2+} cooperativity. These observations strongly suggest that each frequency-dependent step reflects the time required for the dissociation of Ca^{2+} from one of the four binding sites. Thus our model assumes that the transmitter release site contains four independent gates, with kinetics graded from slow, high affinity to fast, low affinity.

Tests of the model

The model was tested in three stages. First we attempted to reproduce the experimental observations on which the model was based: fourth-power kinetics of transmitter release, decline in cooperativity during trains of impulses, and a steplike increase in facilitation with stimulus trains of higher frequency.

Next we checked whether the model was compatible with the outcomes of several published experimental observations of transmitter release. These include: a Ca^{2+} influx to transmitter release latency as short as 0.2 ms; compatibility with stochastic Ca^{2+} channel kinetics; an inverse relation between external Ca^{2+} and the degree of facilitation; facilitation that is not dependent on residual free calcium; and a transmitter release time course that is virtually independent of an increase in the quantal content, whether this is effected by elevating external Ca^{2+} or by paired-pulse facilitation.

Finally, we discuss some experimental tests of the model that could lead to its modification or refutation.

Some of this work has appeared previously in abstract form (Bertram et al. 1995; Stanley et al. 1995).

METHODS

Each release site contains four independent gates (S_1–S_4), with different opening and closing rates. The closing of each gate is Ca^{2+} independent, with S_4 closing most rapidly and S_1 closing most slowly. The kinetic equation for the S_j gate (j = 1, 2, 3, or 4) is

$$Ca + C_j \underset{k_j^-}{\overset{k_j^+}{\rightleftharpoons}} O_j \qquad (1)$$

where Ca is the Ca^{2+} concentration at the release site (μM), C_j is the probability that the gate is closed, and O_j is the probability that it is open (or equivalently, C_j and O_j can be viewed as nondimensional concentrations whose sum is normalized to 1).

Kinetic rates were chosen to produce steps in facilitation (discussed later). Opening rates ($ms^{-1} \cdot \mu M^{-1}$) and closing rates (ms^{-1}) are: $k_1^+ = 3.75 \times 10^{-3}$, $k_1^- = 4 \times 10^{-4}$, $k_2^+ = 2.5 \times 10^{-3}$, $k_2^- = 1 \times 10^{-3}$, $k_3^+ = 5 \times 10^{-4}$, $k_3^- = 0.1$, $k_4^+ = 7.5 \times 10^{-3}$, and $k_4^- = 10$. The dissociation constants for the gates S_1–S_4 are 108 nM, 400 nM, 200 μM, and 1,334 μM, respectively. The time constants for gate closure ($1/k_j^-$) are 2.5 s, 1 s, 10 ms, and 0.1 ms, respectively.

The temporal evolution of open gates is described by the differential equations

$$\frac{dO_j}{dt} = k_j^+ \cdot Ca - O_j/\tau_j \quad j = 1, 2, 3, 4 \qquad (2)$$

where $\tau_j = 1/(k_j^+ \cdot Ca + k_j^-)$. The probability that a release site is activated is

$$R = O_1 \cdot O_2 \cdot O_3 \cdot O_4 \qquad (3)$$

(Equivalently, if we consider the O_j to be concentrations, then we can consider R to be the rate of release per site.) We take the total nondimensional rate of release from a nerve terminal to be the product of R and the number of release sites. For simplicity, we refer to R as release. We neglect depletion of transmitter vesicles.

Equation 2 is solved either analytically or numerically, depending on the stimulus protocol. Numerical computations employ a fourth-order Runge-Kutta method with variable step size. Some simulations employ a Monte Carlo algorithm in conjunction with the numerical differential equation solver.

RESULTS

Two-gate model

In this section we demonstrate that many features of transmitter release can be accounted for by a model with only

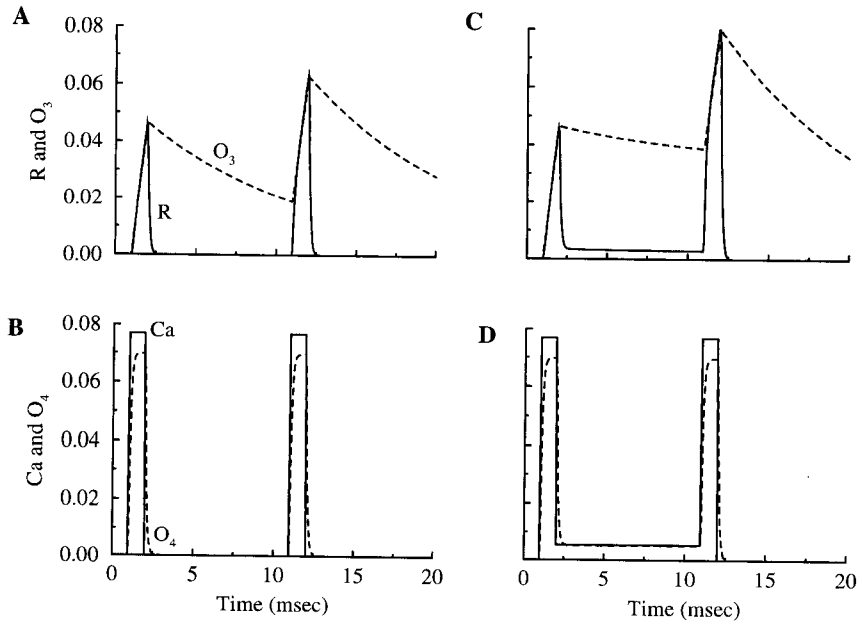

FIG. 1. Release evoked by a 2-pulse protocol at 100 Hz with 1-ms pulse duration and 100-μM pulse amplitude. The 2-gate model is used. In *A* and *B* there is no residual Ca^{2+} between pulses. *A*: open probability of S_3 (------) and release *R* (——) Release has been scaled in *A* and in *C* to allow comparison with the time course of O_3. There is clear facilitation of the 2nd response. *B*: open probability of S_4 (------) and Ca^{2+} concentration (——). *Ca* has been scaled in *B* and in *D*. *C* and *D*: with 7 μM residual Ca^{2+} between pulses, facilitation of the 2nd pulse is enhanced.

two gates (S_3 and S_4) per release site, the simplest case that shows facilitation. In this case $R = O_3 \cdot O_4$. The closing rate of S_3 is such that the gate, once opened, remains open on average for several milliseconds. The closing rate of S_4 is such that the gate closes almost immediately on termination of the Ca^{2+} pulse. The S_3 and S_4 opening rates are such that O_3 rises slowly to its steady state level, whereas O_4 rises rapidly.

We define facilitation of the nth response in a train of stimuli as

$$F^n = \frac{\text{peak release of } n\text{th response}}{\text{peak release of 1st response}} \quad (4)$$

so that $F^n = 1$ corresponds to no facilitation. In Fig. 1, *A* and *B*, we demonstrate how facilitation is produced in the absence of residual Ca^{2+}. Two 100-Hz Ca^{2+} pulses (Fig. 1*B*) provide the stimulation for transmitter release (Fig. 1*A*). Such pulses may be thought of as single-Ca^{2+}-channel openings at a fixed voltage, because domain Ca^{2+} close to the channel reaches equilibrium in microseconds according to simulations of diffusion from a channel with constant influx (Simon and Llinás 1985). The pulse magnitude of 100 μM is consistent with a release site located <50 nm from the channel (Aharon et al. 1994; Llinás et al. 1992). Release evoked by the second pulse is greater than that evoked by the first, with $F^2 = 1.37$. This facilitation occurs because some of the S_3 gates that were opened by the first pulse remain open at the onset of the second pulse (Fig. 1*A*). Residual Ca^{2+} plays no role here, because Ca^{2+} is zero between pulses. The termination of release at the end of each Ca^{2+} pulse is determined by the rapid closure of S_4 (Fig. 1*B*).

Although residual Ca^{2+} is not necessary for facilitation in our model, if present it enhances and prolongs facilitation. This is demonstrated in Fig. 1, *C* and *D*. The stimulation protocol is identical to that above, except that between pulses Ca^{2+} is maintained at 7% of its peak concentration (Fig. 1*D*). The effect of this residual Ca^{2+} is to bind to S_3 between pulses, so that O_3 is higher at the onset of the second pulse. As a result, facilitation is increased to $F^2 = 1.75$.

We return now to the case in which there is no residual Ca^{2+} between successive pulses. In our model, maximum release is attained at the end of a Ca^{2+} pulse, and this value is used in computing facilitation. Because of the fast closing of the S_4 gate, O_4 is identical from pulse to pulse, and thus cancels out in the ratio *Eq. 4*. Thus two-pulse facilitation is the ratio of O_3 values at the end of each pulse. For this pulse protocol, the differential equation for O_3 can be solved analytically, allowing us to derive an expression for facilitation.

For simplicity, we drop the subscript from O_3. Then O at the end of the first pulse ($t = t_P$), denoted O^1, is

$$O^1 = O_\infty \cdot (1 - e^{-t_P/\tau_P}) \quad (5)$$

where $O_\infty = k^+ Ca_P / (k^+ Ca_P + k^-)$ is the steady-state probability that would be achieved in a long pulse to $Ca = Ca_P$. O decays from this level with time constant $\tau_I = 1/k^-$ between pulses, so that

$$O = O^1 \cdot e^{-t_I/\tau_I} \quad (6)$$

at the start of the second pulse, where t_I is the interpulse duration. At the end of the second pulse

$$O^2 = O^1 \cdot e^{-t_I/\tau_I} \cdot e^{-t_P/\tau_P} + O_\infty \cdot (1 - e^{-t_P/\tau_P}) \quad (7)$$

$$= O^1 \cdot e^{-(t_I/\tau_I + t_P/\tau_P)} + O^1 \quad (8)$$

Thus in each interval and following pulse, residual bound Ca^{2+} drops by a factor

$$\alpha = e^{-(t_I/\tau_I + t_P/\tau_P)} \quad (9)$$

and a new increment equal to O^1 is added. Facilitation for this two-pulse protocol is thus

$$F^2 = \frac{O^2}{O^1} = \alpha + 1 \quad (10)$$

This expression allows us to make several observations about the effects of physical parameters on two-pulse facilitation

in the absence of residual Ca^{2+}. First, $F^2 < 2$ because $\alpha < 1$ for any choice of parameters ($F^2 < 8$ for the full model with 3 slow gates). Next, F^2 increases when either pulse duration, t_P, or interpulse duration, t_I, is decreased. Decreasing t_I increases the numerator in *Eq. 4*, whereas decreasing t_P decreases the denominator. Consistent with experimental observations (Rahamimoff 1968; Stanley 1986), decreasing the amplitude of the Ca^{2+} pulse Ca_P, which increases τ_P, also increases facilitation (see Fig. 4). Finally, facilitation is larger for smaller gate opening or closing rates.

The derivation outlined above can be extended to n-pulse facilitation. At the end of the nth pulse, $O^n = O^{n-1}\alpha + O^1$, so $F^n = F^{n-1}\alpha + 1$. This is the recursive form of a geometric series, which sums to

$$F^n = \frac{1 - \alpha^n}{1 - \alpha} \tag{11}$$

In the limit $n \to \infty$,

$$F^{max} = \frac{1}{1 - \alpha} \tag{12}$$

which is the amount of facilitation induced by a long pulse train. Note that F^n converges to F^{max} faster for smaller values of α. Like F^2, F^{max} is greater for larger values of α. Unlike, F^2, F^{max} is unbounded. Thus facilitation generated by this mechanism can be arbitrarily large, depending on the length of the pulse train and the values of physical parameters.

Four-gate model

STEPS IN FACILITATION LINKED TO LOSS OF COOPERATIVITY. We have shown that a model in which each release site contains a single fast and a single slow gate can account for fast facilitation in the absence of residual Ca^{2+}. In this section, we show that many other properties of transmitter release and fast facilitation are accounted for by the full four-gate model (*Eqs. 2* and *3*), in which kinetics are graded from slow, high affinity to fast, low affinity.

Release during a train of four Ca^{2+} pulses at 10 Hz with no residual Ca^{2+} is shown in Fig. 2. Release evoked by the second pulse shows considerable facilitation, with $F^2 = 2.9$, and facilitation increases throughout the train, with $F^3 = 4.3$ and $F^4 = 5.7$ (Fig. 2*A*). The S_3 gate does not contribute to facilitation at this pulse frequency, because the interpulse interval, $t_I = 99$ ms, is considerably longer than the gate closure time constant (Fig. 2*B*). Facilitation is thus due to the accumulation of open S_1 and S_2 gates (Fig. 2*C*).

Because the gates are independent, the contribution each gate makes to facilitation is multiplicative

$$F^n = \left(\frac{1 - \alpha_1^n}{1 - \alpha_1}\right) \cdot \left(\frac{1 - \alpha_2^n}{1 - \alpha_2}\right) \cdot \left(\frac{1 - \alpha_3^n}{1 - \alpha_3}\right) \tag{13}$$

where each α is defined as in *Eq. 9*. Over a long train of pulses ($n \to \infty$), facilitation approaches

$$F^{max} = \left(\frac{1}{1 - \alpha_1}\right) \cdot \left(\frac{1}{1 - \alpha_2}\right) \cdot \left(\frac{1}{1 - \alpha_3}\right) \tag{14}$$

assuming Ca is zero between pulses. In Fig. 3*A*, the dependence of F^{max} on stimulus frequency is plotted. Also shown are the contributions made by the three components $1/(1 - \alpha_1)$, $1/(1 - \alpha_2)$, and $1/(1 - \alpha_3)$.

The most striking feature of Fig. 3*A* is the steplike increase of facilitation with stimulus frequency. At the lowest stimulus frequencies there is no facilitation. At slightly higher frequencies O_1 begins to accumulate, producing the first "step" in facilitation. The F^{max} and $1/(1 - \alpha_1)$ curves coincide because only the S_1 gate contributes to facilitation at these low frequencies. At ~0.5 Hz, O_2 begins to accumulate, producing another step in the facilitation curve. Finally, at ~50 Hz, O_3 begins to accumulate, producing a third step.

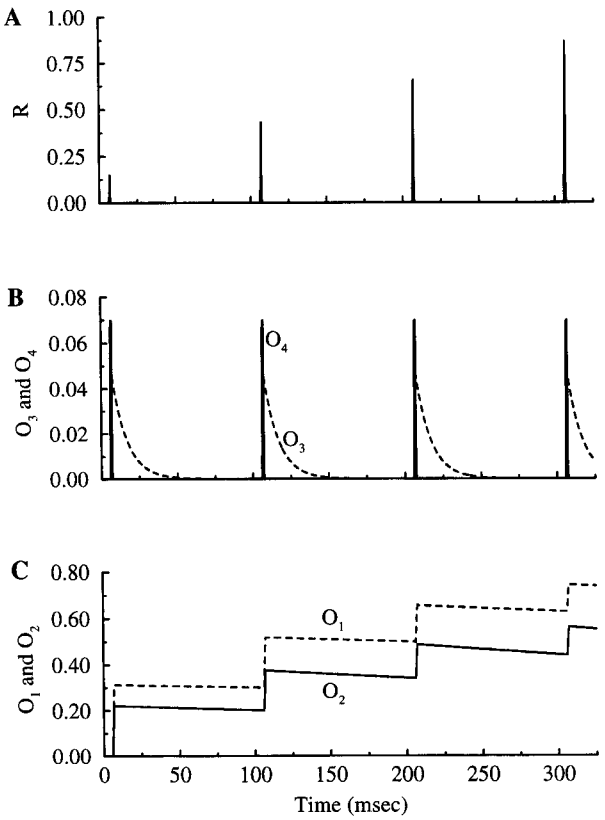

FIG. 2. Release evoked by a 4-pulse protocol at 10 Hz. The 4-gate model is used. Calcium pulse amplitude is 100 μM and pulse duration is 1 ms (not shown). *A*: release (scaled by 700) is facilitated during the stimulus train, in the absence of residual free Ca^{2+}. *B*: O_3 (------) does not contribute to facilitation at this stimulus frequency. *C*: both O_1 (------) and O_2 (——) contribute to facilitation. Total facilitation of each response can be computed from *Eq. 13*. Total facilitation after a long train of pulses at 10 Hz can be computed from *Eq. 14*.

The steplike increase in facilitation corresponds to a steplike decay of Ca^{2+} cooperativity of release (Fig. 3*B*). Thus, during an unfacilitated pulse, $R \propto Ca^{3.9}$ (Fig. 3*B*, *bottom curve*). After a long 5-Hz train of pulses, cooperativity drops to 3.3 due primarily to the accumulation of O_1. Cooperativity drops to 2.7 when stimulus frequency is 20 Hz, because O_1 is almost saturated and there is substantial accumulation of O_2. At 100 Hz, cooperativity drops to 2.2 because now O_1 is saturated, O_2 is approaching saturation, and O_3 has begun to accumulate. At the higher frequencies at which O_3 saturates, cooperativity drops to 1, reflecting the fact that only the fastest gate (S_4) must bind Ca^{2+} to release transmitter. A linkage between facilitation and Ca^{2+} cooperativity has been shown experimentally (Carlson and Jacklet 1986; Stanley 1986).

INVERSE RELATION BETWEEN CALCIUM INFLUX AND FACILITATION. A number of studies have demonstrated a fourth-power relation between transmitter release and calcium. As

shown in Fig. 3*B*, simulations show that $R \propto Ca_P^{3.9}$ when recorded at the end of 2-ms pulses to different concentrations Ca_P from an initial level $Ca = 0$. This near-fourth-power relationship of unfacilitated release can be obtained analytically. From *Eqs. 3* and *5*

$$R = C\alpha_P^4 \cdot \prod_{i=1}^{4} \left[k_i^+ \cdot \tau_{P,i} \cdot (1 - e^{-t_P/\tau_{P,i}}) \right] \quad (15)$$

where $\tau_{P,i} = 1/(k_i^+ Ca_P + k_i^-)$. For pulses of short duration or low Ca_P, $1 - e^{-t_P/\tau_{P,i}} \approx t_P/\tau_{P,i}$, so

$$R \approx Ca_P^4 \cdot t_P^4 \cdot \prod_{i=1}^{4} k_i^+ \quad (16)$$

The total release from a single site during an unfacilitated Ca^{2+} pulse is derived by integrating *Eq. 15* over the duration of the pulse. This expression, plotted in Fig. 4, is approximately fourth order in Ca_P for short pulses or small Ca_P. In contrast to total release, twin-pulse facilitation (*Eq. 13*, $n = 2$) is a decreasing function of Ca_P (Fig. 4). This is because of the saturating effect on the gates of high Ca^{2+} entering during the first pulse, which is reflected in *Eq. 9* as a decrease in the time constants $\tau_{P,i}$ and in *Eq. 13* as a decrease in the factors α_i.

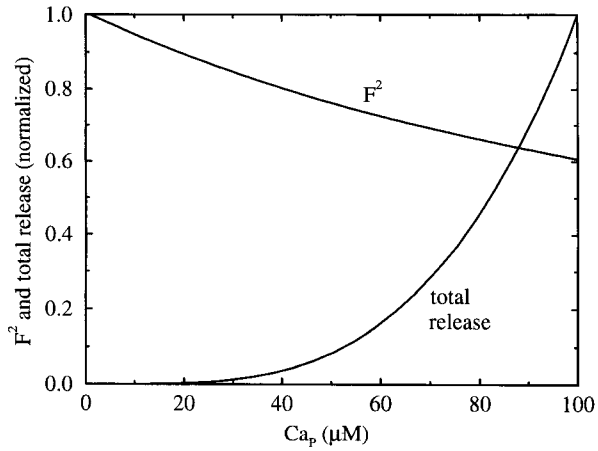

FIG. 4. Total release during a 2-ms Ca^{2+} pulse over a range of pulse magnitudes. There is an approximate 4th-power relationship between total release and Ca_P. In contrast, 2-pulse facilitation at 10 Hz decreases with Ca_P.

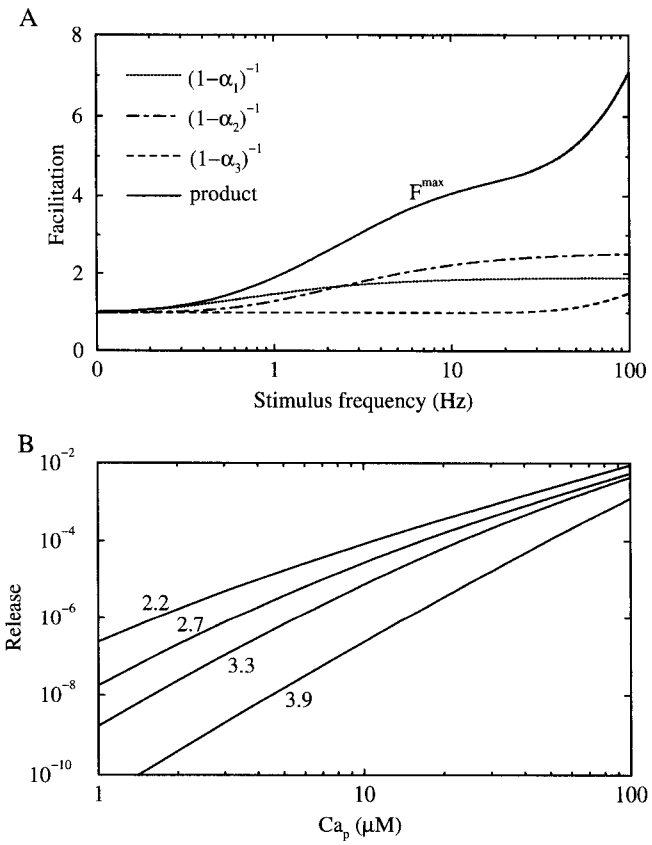

FIG. 3. *A*: steplike increase of facilitation with stimulus frequency. The stimulus here and in *B* is a 2-ms Ca^{2+} pulse to 100 μM. F^{max} is facilitation induced by a long train of pulses at each frequency. Also shown are the components of facilitation due to gate S_1 (· · ·), S_2 (- — -), and S_3 (— — —). To produce steps in facilitation, gate closing rates were chosen to be progressively larger. With this choice of parameters, the afinity of the gates is graded from high (9.3 μM^{-1} for S_1) to low (5×10^{-3} μM^{-1} for S_3). *B*: loss of Ca^{2+} cooperativity accompanying frequency-dependent steps in facilitation. With this logarithmic scale, cooperativity is equal to the slope of the curve. The curve corresponding to an unfacilitated pulse (*bottom curve*) is computed by plotting *Eq. 15* at $t_P = 2$ ms over a range of values of Ca_P. Other curves are obtained in a similar manner by plotting $F^{max} \cdot R$, using *Eqs. 14* and *15*. Cooperativity of an unfacilitated pulse is 3.9 (*bottom curve*), dropping to 3.3, 2.7, and 2.2 following a long train of 5-, 20-, and 100-Hz conditioning stimuli, respectively.

Bulk release and facilitation elicited by stochastic channel openings

STOCHASTIC FORMULA FOR RELEASE AND FACILITATION. In previous sections we were concerned with transmitter release from a single release site, which is proportional to bulk release from the synaptic terminal only if each Ca^{2+} channel opens at the beginning of each presynaptic stimulus and remains open throughout the stimulus. As a first step to a more realistic determination of bulk release evoked by presynaptic voltage pulses, we assume in this section that a channel has a probability p of opening and remaining open throughout the duration of a stimulus. We obtain a formula for the expected value of release from a single release site at the end of a train of n identical stimuli, which is used to determine facilitation associated with this site. The form of this expression for facilitation demonstrates that the properties of the model for single site release discussed in earlier sections are valid in the case of stochastic channel openings. Because expected value is computed, we must interpret C_j and O_j as random variables representing nondimensional concentrations and R as the product of random variables. This interpretation is applied as well in the Monte Carlo simulations below (Figs. 7–9).

For simplicity, we assume that each release site contains the fast gate S_4 and any one of the slow gates, S_{slow}. (The mathematics is more complex if >1 slow gate is considered because slow site binding activity is correlated through Ca^{2+}. This is not a problem with fast gates, which have no memory of previous stimuli.) For either gate, define

$\hat{O}_j = O_j$ at the end of the first stimulus given that the channel opens

$O_j^n = O_j$ at the end of the nth stimulus

Then

$$E[O_j^n] = p \cdot E[O_j^n | \text{channel opens}] + (1 - p) \times E[O_j^n | \text{channel fails to open}] \quad (17)$$

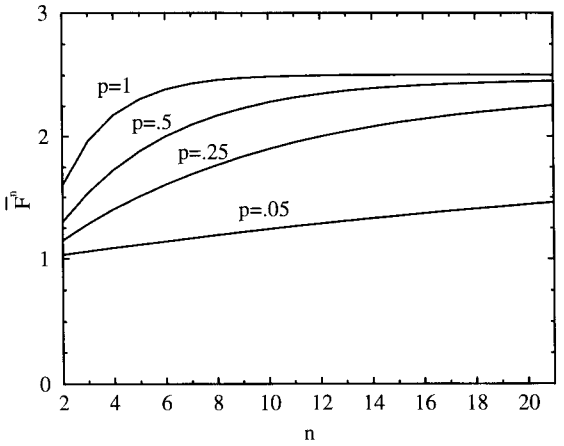

FIG. 5. $\bar{F}^n$ (*Eq. 27*) vs. stimulus number for several values of the channel opening probability p. Stimulus frequency and duration are 100 Hz and 2 ms, respectively. When a channel opens, domain Ca^{2+} concentration rises instantaneously to 100 μM, dropping instantaneously to 0 when the channel closes.

where $E[\cdot]$ is the expected value. If the channel opens, then there is normal decay by α_j (*Eq. 9*) and an increment of $\hat{O}_j$. If the channel fails to open, then there is just decay by $\beta_j = e^{-(t_I+t_P)k_j^-}$. Thus

$$E[O_j^n] = p\cdot(\alpha_j\cdot E[O_j^{n-1}] + \hat{O}_j) + (1-p)\cdot\beta_j\cdot E[O_j^{n-1}] \quad (18)$$

As in the deterministic case ($p = 1$) this gives rise to a simple recursion

$$E[O_j^n] = p\cdot\hat{O}_j + \gamma_j\cdot E[O_j^{n-1}];\quad \gamma_j = p\cdot\alpha_j + (1-p)\cdot\beta_j \quad (19)$$

which is a geometric series with sum

$$E[O_j^n] = p\cdot\hat{O}_j\cdot\left(\frac{1-\gamma_j^n}{1-\gamma_j}\right) \quad (20)$$

Then

$$E[R^n] = p\cdot E[O_{slow}^n\cdot O_4^n|\text{channel opens}] \quad (21)$$

$$= p\cdot E[(\hat{O}_{slow} + \alpha_{slow}\cdot O_{slow}^{n-1})\cdot(\hat{O}_4 + \alpha_4\cdot O_4^{n-1})] \quad (22)$$

$$= p\cdot(\hat{O}_{slow}\cdot\hat{O}_4 + \hat{O}_{slow}\cdot\alpha_4\cdot E[O_4^{n-1}] + \hat{O}_4\cdot\alpha_{slow}\cdot E[O_{slow}^{n-1}] + \alpha_{slow}\cdot\alpha_4\cdot E[O_{slow}^{n-1}\cdot O_4^{n-1}]) \quad (23)$$

$$\approx p\cdot(\hat{O}_{slow}\cdot\hat{O}_4 + \hat{O}_4\cdot\alpha_{slow}\cdot E[O_{slow}^{n-1}]),\quad \text{since } \alpha_4 \approx 0 \quad (24)$$

$$= p\cdot\hat{O}_{slow}\cdot\hat{O}_4\cdot\left[1 + p\cdot\alpha_{slow}\cdot\left(\frac{1-\gamma_{slow}^{n-1}}{1-\gamma_{slow}}\right)\right] \quad (25)$$

Because expected value of facilitation $E[R^n/R^1]$ is undefined (R^1 may be 0), we use as a measure of facilitation

$$\bar{F}^n = \frac{E[R^n]}{E[R^1]} \quad (26)$$

$$= \left[1 + p\cdot\alpha_{slow}\cdot\left(\frac{1-\gamma_{slow}^{n-1}}{1-\gamma_{slow}}\right)\right] \quad (27)$$

This is similar to the expression for facilitation with nonstochastic channel opening, the two being identical when $p = 1$. Thus parameters such as Ca_P, t_P, and t_I have the same effects here as in the cases discussed earlier, so the properties of release and facilitation discussed for nonstochastic channel openings apply also to the case where channel opening is stochastic.

In Fig. 5 we plot *Eq. 27*, using S_2 as the slow gate, to illustrate the effects of stochastic channel openings on facilitation evoked by a train of stimuli. The time course and magnitude are not much affected by p as low as 0.5, and even at $p = 0.05$, facilitation is present.

In the limit $n \to \infty$

$$\bar{F}^{max} = \frac{1-(1-p)\beta_{slow}}{1-\gamma_{slow}} \quad (28)$$

so channel open probability also affects the magnitude of facilitation induced by a long train of stimuli. However, in the limit $k_{slow}^- \to 0$, $\beta_{slow} \to 1$ and $\gamma_{slow} \to p\alpha_{slow} + (1-p)$, so *Eq. 28* becomes

$$\bar{F}^{max} = \frac{1}{1-\alpha_{slow}} \quad (29)$$

which is identical to long train facilitation in the deterministic case (*Eq. 12*). Thus, for gates with a very low unbinding rate, long-train facilitation is approximately the same whether or not Ca^{2+} channel opening is stochastic.

FACILITATION AND RELEASE EVOKED BY VOLTAGE PULSES. We now take the final step to a realistic voltage-clamp simulation by making channel opening and closing rates functions of voltage V. We use the full four-gate model and employ a Monte Carlo algorithm to handle the stochasticity of channel openings. This allows us to investigate tail currents, which are a channel population effect.

We now also need a way to describe the dependence of domain Ca^{2+} on V. Because the domain Ca^{2+} concentration reaches equilibrium within microseconds after the opening of a channel (Simon and Llinás 1985), we assume that it is in equilibrium with membrane potential when the channel is open. In addition, modeling studies suggest that buffer is saturated and may be neglected in the vicinity of the channel (Aharon et al. 1994; Simon and Llinás 1985; Winslow et al. 1994). We therefore assume that Ca is instantaneously proportional to the flux at the mouth of the channel, $Ca = -Ai(V)$ (see also Sherman et al. 1990; Simon and Llinás 1985). We use the Goldman-Hodgkin-Katz formula (Goldman 1943) to describe $i(V)$, the single-channel current (see APPENDIX). Domain Ca^{2+} is then also proportional to Ca_{ex}, the external Ca^{2+} concentration. These proportionality relations are convenient, but not a requirement of our model. Any empirical dependence of Ca on V and Ca_{ex} will work. Indeed, below we confirm selected results with the use of values from a simulation of three-dimensional diffusion near an open channel by Aharon et al. (1994).

Channel opening and closing rates [$k_{ca}^+(V)$ and $k_{ca}^-(V)$, respectively] are fit to data on the squid giant synapse (Llinás et al. 1981a), as described in the APPENDIX. For simplicity we assume that the channel has one open and one closed state. Time is partitioned into bins of duration $\Delta t = 0.01$ ms. At each time $j\Delta t$, the quantities $i(V)$, $k_{ca}^+(V)$ and $k_{ca}^-(V)$ are updated to reflect the appropriate voltage, and the state of each channel is determined. Closed channels open with probability $k_{ca}^+\Delta t$ and open channels close with probability $k_{ca}^-\Delta t$. The voltage dependence of the channel rates is such that during a depolarizing pulse there is a net opening of channels, whereas during a hyperpolarizing pulse there is a net closing of channels. Release from each site is then determined by *Eqs. 2* and *3*, with $Ca = 0$ if the channel is closed and $Ca = -Ai(V)$ if the channel is open. To approxi-

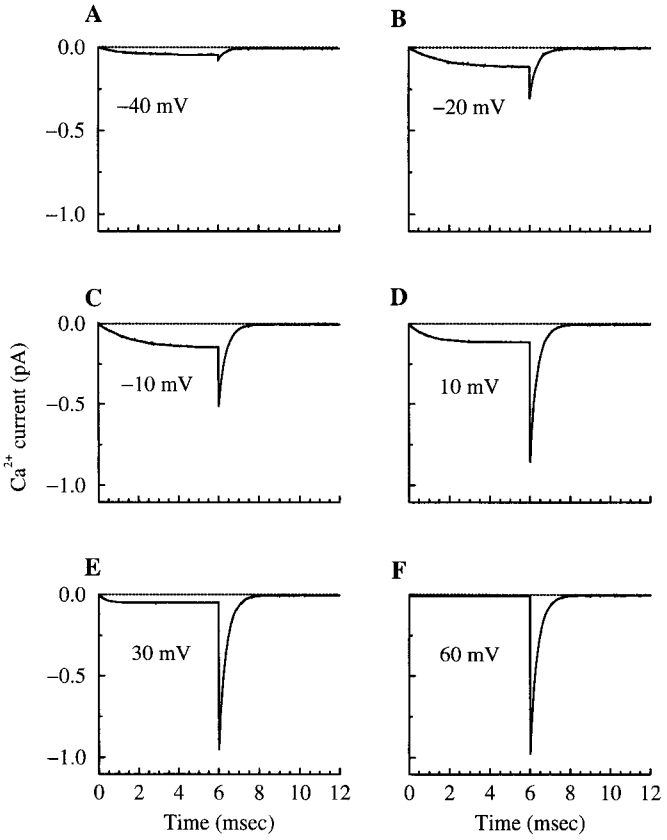

FIG. 6. Expected Ca^{2+} current per channel under simulated voltage clamp. Voltage is initially held at −70 mV, then pulsed at $t = 0$ to various levels for 6 ms and returned to −70 mV. The pulse voltage is indicated in each panel. Expected Ca^{2+} current is the product of the single-channel current $i(V)$ and the fraction of open channels. External calcium concentration: 10 mM.

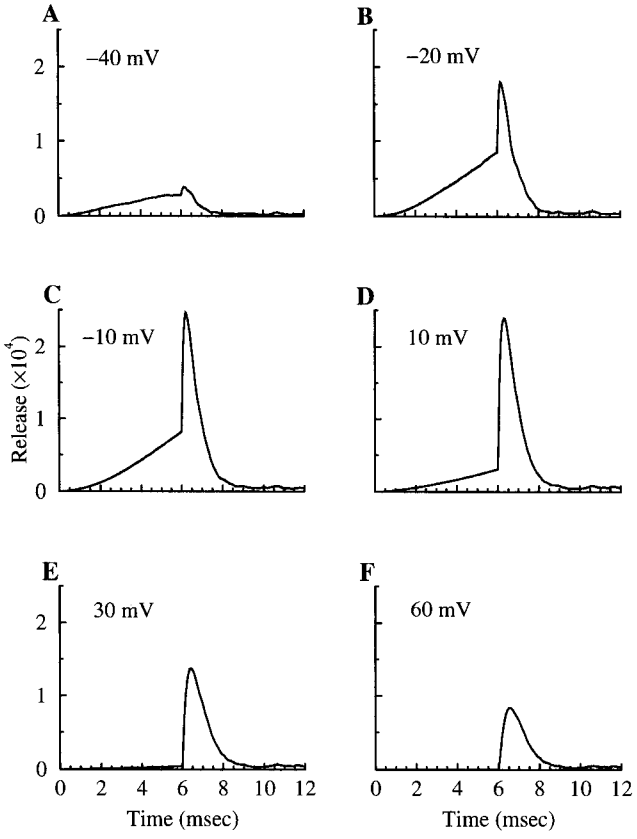

FIG. 7. Expected rate of release per release site in arbitrary units, evoked by the Ca^{2+} currents in Fig. 6. Expected release is proportional to bulk release from the synaptic terminal, assuming no overlap of Ca^{2+} domains. In this and all remaining figures, the system is allowed to reach equilibrium at the membrane holding or resting potential before the start of the simulation. See the APPENDIX for details.

mate the expected single-site release we average over an ensemble of 4,000 release sites, each associated with a calcium channel. The result is proportional to bulk release from the terminal if there is no overlap of calcium domains.

Figures 6 and 7 show Ca^{2+} current and transmitter release during simulated voltage-clamp protocols. At $t = 0$, voltage is stepped from −70 mV to various potentials for 6 ms and returned to −70 mV. From Fig. 6 we see that as the level of depolarization of the pulse is increased, Ca^{2+} current during the pulse first rises (Fig. 6, *A–C*) as more channels are opened, and then falls (Fig. 6, *D–F*) because of the declining single-channel current. This behavior is reflected in the level of release during the pulse, which is low in Fig. 7*A*, maximal in Fig. 7*C*, and almost zero in Fig. 7*F*. The magnitude of the Ca^{2+} current immediately following the pulse (i.e., the tail) rises with higher pulse depolarizations until all Ca^{2+} channels are open, which occurs with pulses to ≥30 mV (Fig. 6, *E* and *F*). One may expect this behavior to be reflected in the magnitude of release during the tail. Instead, tail release first rises (Fig. 7, *A–C*) and then falls (Fig. 7, *D–F*), mimicking the rise and fall of Ca^{2+} current during the pulse.

The reason for the decline in tail release is best exemplified by Fig. 7, *E* and *F*. In either case there is almost no release during the pulse; however, the tail release is larger in Fig. 7*E* than in Fig. 7*F*. Because all channels open in both cases, the difference is due to the larger single-channel current during the pulse at +30 mV. Although this current is too low to evoke significant release, it brings in enough Ca^{2+} to bind the high-affinity gates, leading to a facilitated tail release. This facilitation is not due to buildup of Ca^{2+} near the release site, but rather to the accumulation of high-affinity Ca^{2+}-bound release gates.

These features of release were exhibited in a series of voltage-clamp experiments on the squid giant synapse (Fig. 2, Augustine et al. 1985). The voltage-clamp protocol for these experiments was similar to that used in our simulations, as was the time course of the Ca^{2+} current. The most striking feature of this data is that the tail release first rises and then falls with pulse depolarization, consistent with our simulations.

FACILITATION AND RELEASE EVOKED BY ACTION POTENTIALS. The release of transmitter evoked by action potentials can be simulated with the use of the Monte Carlo technique described in the previous section, with membrane potential changing in accordance with the dynamics of ion flux through the synaptic membrane. We simulate an action potential using the Hodgkin-Huxley equations (see APPENDIX). For simplicity, we assume that membrane potential is affected only by the flow of Na^+ and K^+ ions, so that Ca^{2+}

current is affected by, but does not affect, membrane potential. Thus, at each time step the membrane potential is updated according to the Hodgkin-Huxley equations, then the Ca^{2+}-channel opening and closing rates are updated to reflect the new voltage and any channel transitions are made, and finally release of transmitter from each release site is determined according to *Eqs. 2* and *3*.

Figure 8*A* shows release evoked by 10 successive action potentials, with action potentials superimposed. At the peak of each impulse there is a small "bump" of increased transmitter release, due to the opening of calcium channels. However, it is not until the membrane repolarizes that the single-channel calcium influx is great enough to bind the S_4 gate and evoke significant release. Thus peak release occurs after the peak voltage, as observed experimentally (Llinás et al. 1982). There is facilitation throughout the train, due primarily to the accumulation of bound S_1 and S_2 gates. This accumulation of bound calcium increases not only the evoked release, but also the spontaneous release between impulses. This can be observed both in Fig. 8*A* and in Fig. 8*B*, where the responses to the 1st and 10th impulses are superimposed and normalized by their peak values. It is clear from this that the spontaneous release scales as the evoked release. A similar increase in spontaneous release has been observed

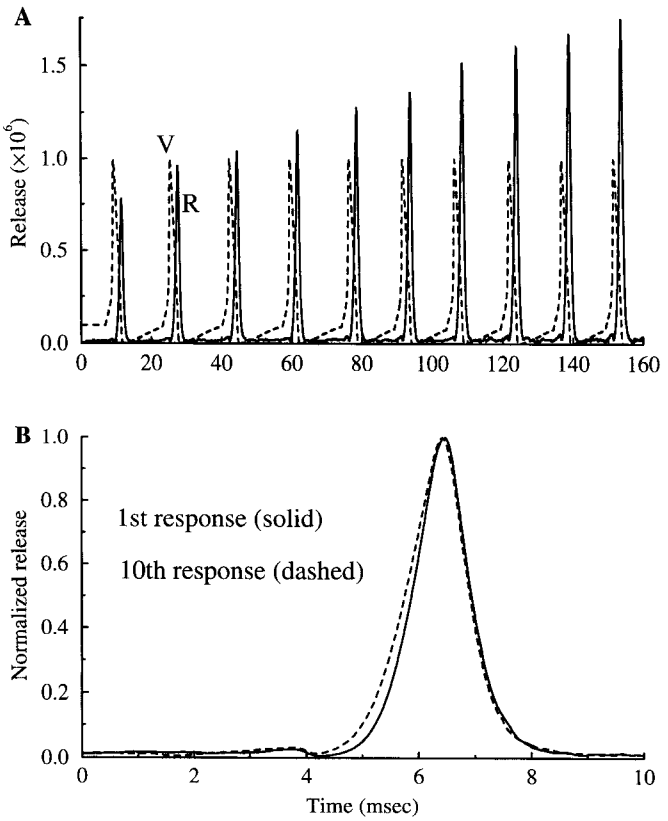

FIG. 8. *A*: expected rate of release per release site in arbitrary units, evoked by 10 successive action potentials. Even with stochastic Ca^{2+} channel openingss, there is significant facilitation throughout the train of impulses. Consistent with experiments, peak release occurs after peak depolarization. Membrane potential (------) is normalized. External calcium concentration is 1 mM, consistent with Datyner and Gage (Fig. 9, 1980). *B*: responses evoked by the 1st impulse (——) and the 10th impulse (------) from *A* are largely invariant when superimposed and normalized. Compare with Fig. 9 of Datyner and Gage (1980).

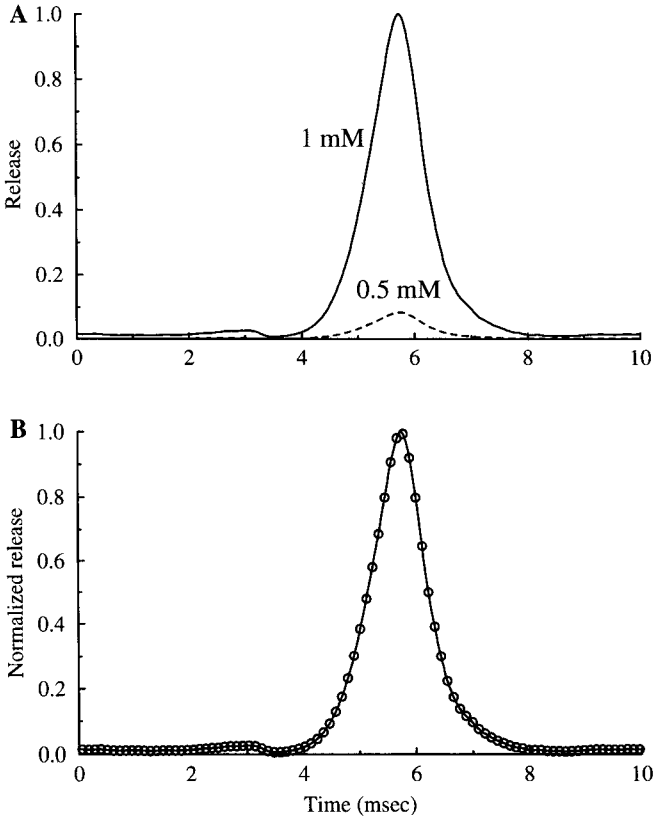

FIG. 9. *A*: expected rate of release per release site in arbitrary units, evoked by an action potential in 1 mM external Ca^{2+} (——) and 0.5 mM external Ca^{2+} (------). The nonlinear response to the change in calcium concentration is consistent with experiments. Release has been scaled by the maximum release in 1 mM calcium. *B*: responses in 1 mM external Ca^{2+} (——) and 0.5 mM external Ca^{2+} (○) are indistinguishable when superimposed and normalized to their peaks. Compare with Fig. 8 of Datyner and Gage (1980).

in experiments (Andreu and Barrett 1980; Rahamimoff and Yaari 1973; Zengel and Magleby 1981).

Figure 8*B* also demonstrates the near-invariance of the normalized time course of release for unfacilitated and facilitated pulses. This is consistent with experiments by Datyner and Gage (1980) showing invariance of the first three responses to a train of impulses of similar frequency. The amount of facilitation exhibited in Fig. 8*A* is also similar to that reported in these experiments.

In separate experiments, Datyner and Gage showed that the amount of transmitter released by an action potential in 1 mM external Ca^{2+} is much greater than the amount released in 0.5 mM external Ca^{2+}. Our model also shows this behavior (Fig. 9*A*), the large increase in release reflecting the nonlinear relationship between Ca^{2+} and release discussed earlier. Despite the great difference in release magnitude, the two release time courses in Fig. 9*A* are indistinguishable when normalized and superimposed (Fig. 9*B*), consistent with experiments (Datyner and Gage 1980). The model predicts a similar invariance during voltage-clamp depolarizations.

One might think that these simulations are biased by our assumption that domain Ca^{2+} is proportional to the single-channel Ca^{2+} current and to the concentration of external Ca^{2+}. To investigate this possibility we simulated release

during a 1-ms depolarization to either −30 or 0 mV from −70 mV, using for *Ca* the values computed by Aharon et al. (1994, Fig. 8) with a full diffusion model, assuming a distance of 50 nm between Ca^{2+} channel and release site and external Ca^{2+} levels of 1 and 10 mM. Here *Ca* is not proportional to either Ca^{2+} current or external Ca^{2+}. Although not perfectly superimposible, the normalized time courses remain substantially invariant to changes in external Ca^{2+}.

DISCUSSION

We have presented a model for synaptic transmitter release and fast facilitation that is motivated by experimental findings that release can be evoked by single Ca^{2+}-channel openings (Stanley 1993; Yoshikami et al. 1989) and that there is a fourth-power relationship between release and internal Ca^{2+} (Landò and Zucker 1994) or external Ca^{2+} (Andreu and Barrett 1980; Dodge and Rahamimoff 1967) that decays in a steplike fashion with stimulus frequency (Stanley 1986; Liu and Stanley 1995). Thus we have based our model on only three basic elements: single-domain secretion, four Ca^{2+}-activated gates, and a range of decay rates of these gates. In this model, the time course of release is determined by the kinetics of Ca^{2+} binding and unbinding to gates at the release sites, rather than the rates of free Ca^{2+} accumulation and diffusion (Fig. 1). The gates, which are graded from fast, low affinity, to slow, high affinity, take on different roles in the release process. Because of the low affinity of gate S_4, calcium concentration must be high to evoke release. The fast closing rate of this gate ensures that release terminates quickly after closure of an adjacent Ca^{2+} channel. The time course of the onset of release is, however, determined by the binding of Ca^{2+} to the slower, higher-affinity gates S_1-S_3. Because the release time course is sculpted by the gate kinetics, it is remarkably invariant to changes in external Ca^{2+} and prior facilitation-inducing stimulation (Figs. 8 and 9). An earlier model based entirely on the diffusion of Ca^{2+} (Zucker and Fogelson 1986) lacked this feature of invariance, a critical test for any proposed release mechanism (Datyner and Gage 1980; Parnas et al. 1989).

Despite the simplicity of our model, it can reproduce a wide range of transmitter release properties. This simplicity was achieved by intentionally omitting other nerve terminal properties that may ultimately have to be included to reproduce some of the subtleties of nerve terminal function. We make the following assumptions: calcium influx is linearly related to external calcium; there is no delay between Ca^{2+} binding and activation of secretion; and the release sites do not inactivate or have a refractory period due, for example, to vesicle depletion. The most important simplifying assumption, however, is that transmitter release is gated by single Ca^{2+} domains, so that release from each site depends only on the past history of the corresponding Ca^{2+} channel. Because the opening of Ca^{2+} channels is stochastic, a given channel may open only on a small fraction of stimuli during a presynaptic train. We have shown that significant facilitation can be achieved even when the probability of channel opening is low (Figs. 5 and 8).

A necessary consequence of the single-channel domain hypothesis is that residual free Ca^{2+} is neglected. There is compelling experimental evidence supporting this simplification. Delaney and Tank (1994) showed that during an impulse train of moderate frequency, free Ca^{2+} accumulated in the crayfish opener neuromuscular junction. However, substantial accumulation occurred only after facilitation was present, demonstrating that residual free Ca^{2+} plays at most a supportive role in facilitation. Winslow et al. (1994) showed that elimination of free Ca^{2+} between impulses with bis-(*o*-aminophenoxy)-*N,N,N′,N′*-tetraacetic acid or ethylene glycol-bis(*β*-aminoethyl ether)-*N,N,N′,N′*-tetraacetic acid had little or no effect on facilitation, even at a high stimulus frequency (but see Kamiya and Zucker 1994). Consistent with these data, our model exhibits a high degree of facilitation without residual free Ca^{2+}. If present, however, residual free Ca^{2+} both enhances and prolongs facilitation by binding to high-affinity sites between stimuli (Fig. 1). Thus the model is compatible with the enhancement of release that occurs after prolonged stimulus trains, termed posttetanic potentiation, that has been attributed to cytoplasmic free Ca^{2+} (Delaney and Tank 1994; Delaney et al. 1989; Regehr et al. 1994).

A previous model has attempted to account for transmitter release and facilitation by including multiple Ca^{2+} binding sites, one of which was slow, in the release mechanism (Yamada and Zucker 1992). However, substantial facilitation occurs with this model only if the site continues to be loaded with residual free Ca^{2+} that persists after the conditioning impulse, in contrast to the experimental data described above.

There is ample evidence for several components of fast facilitation, each operating on a different time scale (see Magleby 1987 for review). It was shown that facilitation increases in three distinct steps with increasing stimulus frequency (Stanley 1986), and Winslow et al. (1994) have shown that facilitation decays in three distinct phases following a train of impulses. These data are consistent with the mechanism of facilitation implicit in our model, in which Ca^{2+} slowly unbinds from three gates at each release site, each gate releasing its Ca^{2+} at a different rate. The fastest gate essentially works as a switch for release and therefore does not contribute to facilitation. Also consistent with this mechanism is the observation (Stanley 1986) that steps in the frequency dependence of facilitation are linked to a steplike decay in Ca^{2+} cooperativity (Fig. 3). Each facilitation step occurs at a stimulus frequency corresponding to the unbinding rate of one of the slow gates, so that fewer calcium ions are needed to evoke release during a facilitated pulse. It is hard to envision how any model in which facilitation is based on residual free Ca^{2+} (Parnas and Segel 1984; Yamada and Zucker 1992; Zucker and Fogelson 1986) can account for this multiphasic behavior.

With our model we can make several predictions and observations regarding spontaneous release of transmitter and the effects on release and facilitation of changing the level of resting free calcium, through manipulations of external Ca^{2+} or hyperpolarizing prepulses. Spontaneous release is often observed to increase during a train of impulses (Andreu and Barrett 1980; Rahamimoff and Yaari 1973; Zengel and Magleby 1981). In our model, calcium influx during impulses increases the amount of bound Ca^{2+}, which can increase spontaneous release in at least two ways. First, it may be possible for release to occur when fewer than four of the

gates at a site are bound, in which case spontaneous release will be elevated under any conditions where facilitation is evident (a possibility that would require an extension of our model). With this mechanism spontaneous release will remain elevated even if external Ca^{2+} is removed from the bath. A second source of elevated spontaneous release requires no special assumptions, only that there is a background level of spontaneous Ca^{2+} channel openings. This mechanism is responsible for the elevated spontaneous release in Fig. 8. Although the probability that a Ca^{2+} channel opens after an impulse is no greater than that before the impulse, the residual bound Ca^{2+} increases the probability that such an event will evoke release. In our model, the elevated spontaneous release decays in three phases between impulses and after the last impulse in the train because of the three dissociation rates of the slow gates. Zengel and Magleby (1981) found that decay of spontaneous release occurred with four time scales, one of which they attributed to the decay of potentiation, one to augmentation, and two to facilitation. The latter three time scales are similar to the dissociation time constants for our S_1, S_2, and S_3 gates, so it is likely that three of the four phases of decay observed by Zengel and Magleby are due to the dissociation of Ca^{2+} from these gates. The other phase of decay has been attributed to the decay of posttetanic potentiation, which is thought to depend on residual free Ca^{2+} (Delaney and Tank 1994; Delaney et al. 1989), and is beyond the scope of the present work.

The release machinery is sensitive to external Ca^{2+} concentrations even when there are no action potentials. Even though the open probability of a Ca^{2+} channel is low at the resting membrane potential, Ca^{2+} from infrequent channel openings can bind to and possibly saturate high-affinity Ca^{2+} binding sites if the unbinding rates are sufficiently low and if the influx of Ca^{2+} through an open channel is sufficiently high. Thus experimental conditions in which external Ca^{2+} concentration is high may mask the influence of the high-affinity binding sites. We predict that there will be lower Ca^{2+} cooperativity and facilitation and fewer steps in the frequency dependence of facilitation under high-resting-calcium conditions.

Changes in the resting calcium level could account for the observation that a hyperpolarizing prepulse decreases the transmitter release evoked by a pulse depolarization (Datyner and Gage 1982; Molgó and Thesleff 1982; Parnas et al. 1986b). During the hyperpolarization the average number of open Ca^{2+} channels is reduced, resulting in a reduction in the level of resting calcium. As a consequence, Ca^{2+} unbinds from the slow gates, decreasing the subsequent depolarization-induced release. We predict that this will also result in an increase in twin-pulse facilitation, as will any manipulation that decreases the resting level of bound calcium (see Parnas et al. 1986b for some evidence supporting this prediction).

Elevated external Ca^{2+} affects both the level of internal resting calcium and the magnitude of Ca^{2+} influx during a depolarization. The consequences of these two effects for Ca^{2+} cooperativity of release and fast facilitation are hard to disentangle in an experimental setting. We have separated the latter effect from the former by assuming in the mathematical analysis and in a series of simulations that internal calcium is not present before and between stimuli (Figs. 1–5). Under these conditions, we showed that increasing the amount of Ca^{2+} influx during a stimulus reduces facilitation by increasing release elicited by the first pulse (Fig. 4). However, cooperativity during an unfacilitated pulse is approximately fourth order over a wide range of Ca^{2+} influx values. In addition, an equal number of steps in the frequency dependence of facilitation should be observed regardless of the amplitude of Ca^{2+} influx.

It is also possible that raising external Ca^{2+} will substantially broaden presynaptic action potentials because of the increased Ca^{2+} current across the membrane. We have investigated this possibility by including Ca^{2+} current in the spike-generating component of our model (see APPENDIX). If the Ca^{2+} conductance is large, then the action potentials become broader with a pronounced shoulder. In this case, changing external Ca^{2+} (from 0.5 to 1.0 mM, for example, as was done in Fig. 9) has a substantial effect on the normalized time course of release. Raising Ca^{2+} both broadens the release time course and increases its latency, destroying the invariance reported both experimentally and in Fig. 9. Similar effects on release were shown in experiments where action potentials were broadened with K^+ channel blockers (Augustine 1990; Datyner and Gage 1980), and we can reproduce these effects by decreasing the potassium conductance in the model. There is, however, much evidence that Ca^{2+} current in the synaptic terminal is small relative to the Na^+ current, so that its effect on the action potential is minor (Llinás et al. 1981a,b; Stanley 1986). Llinás et al. (1981a) compute the Ca^{2+} current density to be $\sim 1/20$ the size of the Na^+ current density in the squid giant synapse. If this relation is used in our model, then changing external Ca^{2+} has little effect on the action potential and the normalized time course of release remains invariant (not shown).

Although our model is intended primarily to describe release during brief depolarizations such as action potentials, we have applied it to a series of simulated voltage-clamp protocols in which the membrane is depolarized for a long period of time (Figs. 6 and 7). The goal here is to understand which properties of release depend primarily on the properties of the release site and which depend also on the distribution of Ca^{2+} channels. Consistent with experiments (Augustine et al. 1985; Llinás et al. 1981b), release elicited during a voltage pulse first increased and then decreased with depolarization, mimicking the behavior of the bulk Ca^{2+} current. This behavior was also exhibited by release evoked by the Ca^{2+} tail current, even though the tail current rises continuously with depolarization until it saturates. This loss of correlation between tail current and tail release was observed by Augustine et al. (1985) and attributed to facilitation taking place during the pulse. Our simulations provide a physical basis for this phenomenon. At some positive voltages single-channel Ca^{2+} influx during a pulse may not be sufficient to bind to the low-affinity gate and evoke release, but may be sufficient to open the higher-affinity gates and thus facilitate the tail release. Facilitation during the pulse will be less pronounced at voltages closer to the Ca^{2+} reversal potential, resulting in a decline in tail release at high voltages. This is particularly evident in Fig. 7, *E* and *F*.

One property of the squid giant synapse not reproduced by our model is that during long depolarizations the release is higher at more depolarized voltages, when channel opening

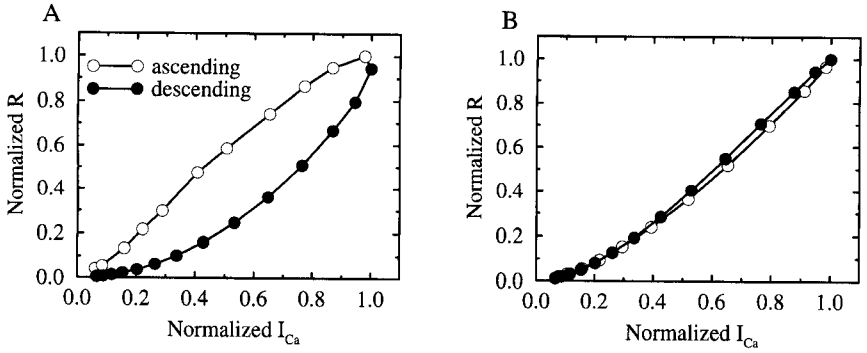

FIG. 10. Transfer curves relating the magnitude of Ca^{2+} current and release at the end of 6-ms depolarizations to the potentials used in Figs. 6 and 7. As before, holding potential is −70 mV. *A*: simulation with 1 Ca^{2+} channel per release site. The "ascending" arm of the curve, corresponding to pulses to −5 mV and below (○), lies above the "descending" arm, corresponding to larger depolarizations (●). *B*: simulation with 20 Ca^{2+} channels per release site. The descending arm now lies above the ascending arm, consistent with data from the squid giant synapse.

probability is high, than at lower voltages that induce the same bulk Ca^{2+} current (Augustine et al. 1985; Llinás et al. 1981b). The opposite is seen in Fig. 10*A*, where release at the end of the 6-ms depolarizations in Fig. 7 is plotted against bulk Ca^{2+} current. We have extended the model so that multiple Ca^{2+} channels are present local to each binding site, assuming for simplicity that they are equidistant from the site so that diffusion of Ca^{2+} may be neglected. We have found that increasing the number of channels enhances the release elicited by pulses to high voltages more than that elicited by pulses to low voltages because of the overlap of Ca^{2+} domains, as suggested in earlier modeling studies (Simon and Llinás 1985; Zucker and Fogelson 1986). Thus, consistent with the squid data, release is greater at high voltages than at lower voltages when there are 20 channels per release site (Fig. 10*B*), suggesting that there is considerable overlap of Ca^{2+} domains in the squid synapse. It remains to be seen whether this relation persists in other preparations where the ratio of Ca^{2+} channels to release sites is lower (Haydon et al. 1994). Besides highlighting a limitation in the single-Ca^{2+} domain hypothesis, our analysis allows us to draw the important conclusion that one role of overlapping Ca^{2+} domains is to accentuate depolarization-evoked release relative to spontaneous release. However, stronger support for this conclusion awaits a more detailed study in which the specific geometry of Ca^{2+} channels and release sites is taken into account. Previous modeling studies have shown the importance of this consideration (Bennett et al. 1995; Simon and Llinás 1985; Zucker and Fogelson 1986).

With regard to robustness to parameter selection, the binding and unbinding rates for the four gates were chosen to produce frequency-dependent steps in facilitation. There are many parameter combinations satisfying this requirement. For example, the fastest gate, S_4, does not influence the facilitation steps as long as it remains fast, so the release probability can be greatly increased or decreased by changing the kinetic rates of this gate. However, some parameter choices are better than others at reproducing other properties of release or facilitation. In particular, invariance is somewhat sensitive to the choice of kinetic rates for both slow and fast gates. These properties, therefore, help constrain the range of parameter values that can be used in the model.

Calcium binding could be more complex than the independent model considered here. The four sites could be linked and sequential or they could be identical and cooperative such that on Ca^{2+} binding the affinities change. At present the identity of the Ca^{2+} binding trigger protein at the release site is not known. One candidate is the integral secretory vesicle protein synaptotagmin. This protein has been shown to have Ca^{2+} binding sites, to bind lipids in a calcium-sensitive manner, and to be important, if not obligatory, in transmitter release. Synaptotagmin, in the presence of lipid, can bind up to four calcium ions, with 50% bound at ~10 μM (Brose et al. 1992; Davletov and Südhof 1993). It is fairly easy to alter the model so that Ca^{2+} binding to the S_3 and S_4 gates can be attributed to synaptotagmin simply by adjusting the binding rates so that the dissociation constants are 10 μM. However, it is more difficult to attribute the S_2 gate to this protein while the S_1 gate cannot practically have such a low affinity and still function as described. Thus, if the published Ca^{2+} affinity of synaptotagmin is an accurate representation of synaptotagmin Ca^{2+} binding in situ, then our model suggests that a synaptotagmin variant of some other protein(s) with much higher Ca^{2+} affinity must also be involved in the secretory mechanism. One possibility is that there are two proteins each of which must bind two calcium ions for vesicular secretion to proceed. One has two low-affinity sites with rapid Ca^{2+} unbinding and is primarily involved in gating secretion, whereas the other has two high-affinity sites with slow Ca^{2+} unbinding and is important in the short-term modulation of transmitter release.

APPENDIX

For the single-channel Ca^{2+} current we use the Goldman-Hodgkin-Katz formula (Goldman 1943), neglecting the effect of intracellular Ca^{2+} at the inner mouth of the channel

$$i(V) = \hat{g}_{Ca} P \frac{2FV}{RT}\left[\frac{Ca_{ex}}{1 - \exp(2FV/RT)}\right] \qquad (A1)$$

Here $\hat{g}_{Ca}$ is the single-channel conductance, P converts concentration to membrane potential, Ca_{ex} is external Ca^{2+} concentration, and RT/F is the thermal voltage (26.7 mV). We use $\hat{g}_{Ca}$ = 12 pS and P = 1.6 mV/mM. Because each release site is assumed to be adjacent to a Ca^{2+} channel, a good approximation for Ca^{2+} concentration at the release site is $Ca = -Ai(V)$, the negative sign being necessary because the current is inward. For A we use the value 0.1 μM/fA, so that Ca rises to ~100 μM when a Ca^{2+} channel opens when Ca_{ex} = 10 mM at −70 mV.

The voltage-dependent Ca^{2+} channel opening and closing rates [$k_{ca}^{+}(V) = 0.6e^{1.45V/26.7}$ and $k_{ca}^{-}(V) = 0.2e^{-V/26.7}$, respectively] were chosen so that the steady-state activation function, $k_{ca}^{+}/(k_{ca}^{+} + k_{ca}^{-})$, matches that measured in the squid giant synapse (Llinás et al. 1981a). They were also chosen so that the channel time constant, $1/(k_{ca}^{+} + k_{ca}^{-})$, is of the right magnitude to match experimental voltage-clamp current records (Llinás et al.

1981a,b). We assume that a channel opens on the binding of a single "activation particle."

In simulations of release evoked by action potentials we use the Hodgkin-Huxley equations (Hansel et al. 1993; Hodgkin and Huxley 1952)

$$C_m \frac{dV}{dt} = -[\bar{g}_{Na} m^3 h(V - V_{Na}) + \bar{g}_K n^4 (V - V_K) + \bar{g}_{leak}(V - V_{leak}) - I_{app}] \quad (A2)$$

$$\frac{dm}{dt} = [m_\infty(V) - m]/\tau_m(V) \quad (A3)$$

$$\frac{dn}{dt} = [n_\infty(V) - n]/\tau_n(V) \quad (A4)$$

$$\frac{dh}{dt} = [h_\infty(V) - h]/\tau_h(V) \quad (A5)$$

where $m_\infty(V) = \alpha_m/(\alpha_m + \beta_m)$, $\tau_m(V) = 1/(\alpha_m + \beta_m)$ (similarly for n_∞, h_∞, τ_n, and τ_h), and $\alpha_m = 0.1(V + 40)/[1 - e^{-(V+40)/10}]$, $\beta_m = 4e^{-(V+65)/18}$, $\alpha_n = 0.01(V + 55)/[1 - e^{-(V+55)/10}]$, $\beta_n = 0.125\, e^{-(V+65)/80}$, $\alpha_h = 0.07\, e^{-(V+65)/20}$, and $\beta_h = 1/[1 + e^{-(V+35)/10}]$. Here m, n, and h are gating variables; C_m is the membrane capacitance; $\bar{g}_{Na}$, $\bar{g}_K$, and $\bar{g}_{leak}$ are the maximum conductances for the sodium, potassium, and leak currents; and V_{Na}, V_K, and V_{leak} are the corresponding reversal potentials. Parameter values are: $C_m = 1\ \mu F \cdot cm^{-2}$, $\bar{g}_{Na} = 120\ mS \cdot cm^{-2}$, $\bar{g}_K = 36\ mS \cdot cm^{-2}$, $\bar{g}_{leak} = 0.3\ mS \cdot cm^{-2}$, $V_{Na} = 50$ mV, $V_K = -77$ mV, and $V_{leak} = -54$ mV. To induce an action potential a current of $I_{app} = 10\ \mu A \cdot cm^{-2}$ was applied for 2 ms. In Figs. 8 and 9 we make the simplifying assumption that Ca^{2+} current is affected by, but does not affect, membrane potential. In one simulation discussed but not shown we add a Ca^{2+} current, $I_{Ca} = \bar{g}_{Ca} x i(V)$, to *Eq.* A2. Here $i(V)$ is the current through a single open Ca^{2+} channel, x is the mean fraction of open channels, and $\bar{g}_{Ca}$ is the maximum Ca^{2+} conductance ($\bar{g}_{Ca} = 1.2$, or $10\ mS \cdot cm^{-2}$).

At a fixed membrane potential the equilibrium ensemble average of O_j for gate S_j is approximately $O_j = k_j^+ Ca/(k_j^+ Ca + k_j^-)$, where $Ca = -Ai(V)\ k_{ca}^+/(k_{ca}^+ + k_{ca}^-)$, the average equilibrium calcium concentration per release site. At $V = -70$ mV, $Ca \approx 70$ nM in 1 mM external Ca^{2+} (Ca varies linearly with Ca_{ex}). We use these expressions as initial conditions in all Monte Carlo simulations.

We thank A. N. Van Driessche, a Summer student at the National Institutes of Health, for help in performing numerical simulations.

Address for reprint requests: R. Bertram, National Institute of Diabetes and Digestive and Kidney Diseases, NIH, Mathematical Research Branch, BSA Bldg., Suite 350, Bethesda, MD 20814.

Received 7 April 1995; accepted in final form 1 November 1995.

REFERENCES

AHARON, S., PARNAS, H., AND PARNAS, I. The magnitude and significance of Ca^{2+} domains for release of neurotransmitter. *Bull. Math. Biol.* 56: 1095–1119, 1994.

ANDREU, R. AND BARRETT, E. F. Calcium dependence of evoked transmitter release at very low quantal contents at the frog neuromuscular junction. *J. Physiol. Lond.* 308: 79–97, 1980.

AUGUSTINE, G. J. Regulation of transmitter release at the squid giant synapse by presynaptic delayed rectifier potassium current. *J. Physiol. Lond.* 431: 343–364, 1990.

AUGUSTINE, G. J., ADLER, E. M., AND CHARLTON, M. P. The calcium signal for transmitter secretion from presynaptic nerve terminals. *Ann. NY Acad. Sci.* 635: 365–381, 1991.

AUGUSTINE, G. J., CHARLTON, M. P., AND SMITH, S. J. Calcium entry and transmitter release at voltage-clamped nerve terminals of squid. *J. Physiol. Lond.* 367: 163–181, 1985.

BALNAVE, R. J. AND GAGE, P. W. On facilitation of transmitter release at the toad neuromuscular junction. *J. Physiol. Lond.* 239: 657–675, 1974.

BENNETT, M. R., GIBSON, W. G., AND ROBINSON, J. Probabilistic secretion of quanta: spontaneous release at active zones of varicosities, boutons, and endplates. *Biophys. J.* 69: 42–56, 1995.

BERTRAM, R., SHERMAN, A., AND STANLEY, E. The single domain/bound calcium hypothesis of transmitter release and facilitation (Abstract). *Biophys. J.* 68: 396, 1995.

BITTNER, G. D. AND SCHATZ, R. A. An examination of the residual calcium theory for facilitation of transmitter release. *Brain Res.* 210: 431–436, 1981.

BLUNDON, J. A., WRIGHT, S. N., BRODWICK, M. S., AND BITTNER, G. D. Residual free calcium is not responsible for facilitation of neurotransmitter release. *Proc. Natl. Acad. Sci. USA* 90: 9388–9392, 1993.

BROSE, N., PETRENKO, A. G., SÜDHOF, T. C., AND JAHN, R. Synaptotagmin: a calcium sensor on the synaptic vesicle surface. *Science Wash. DC* 256: 1021–1025, 1992.

CARLSON, C. G. AND JACKLET, J. W. The exponent of the calcium power function is reduced during steady state facilitation in neuron R_{15} of *Aplysia*. *Brain Res.* 376: 204–207, 1986.

DATYNER, N. B. AND GAGE, P. W. Phasic secretion of acetylcholine at a mammalian neuromuscular junction. *J. Physiol. Lond.* 303: 299–314, 1980.

DATYNER, N. B. AND GAGE, P. W. Secretion of acetylcholine in response to graded depolarization of motor nerve terminals. *J. Physiol. Paris* 78: 412–416, 1982.

DAVLETOV, B. A. AND SÜDHOF, T. C. A single C_2 domain from synaptotagmin I is sufficient for high affinity Ca^{2+}/phospholipid binding. *J. Biol. Chem.* 268: 26386–26390, 1993.

DELANEY, K. R. AND TANK, D. W. A quantitative measurement of the dependence of short-term synaptic enhancement on presynaptic residual calcium. *J. Neurosci.* 14: 5885–5902, 1994.

DELANEY, K. R., ZUCKER, R. S., AND TANK, D. W. Calcium in motor nerve terminals associated with posttetanic potentiation. *J. Neurosci.* 9: 3558–3567, 1989.

DODGE, F. A., JR. AND RAHAMIMOFF, R. Co-operative action of calcium ions in transmitter release at the neuromuscular junction. *J. Physiol. Lond.* 193: 419–432, 1967.

FOGELSON, A. L. AND ZUCKER, R. S. Presynaptic calcium diffusion from various arrays of single channels. *Biophys. J.* 48: 1003–1017, 1985.

GOLDMAN, D. E. Potential, impedance, and rectifications in membranes. *J. Gen. Physiol.* 27: 36–60, 1943.

HANSEL, D., MATO, G., AND MEUNIER, C. Phase dynamics for weakly coupled Hodgkin-Huxley neurons. *Europhys. Lett.* 23: 367–372, 1993.

HAYDON, P. G., HENDERSON, E., AND STANLEY, E. F. Localization of individual calcium channels at the release face of a presynaptic nerve terminal. *Neuron* 13: 1275–1280, 1994.

HODGKIN, A. L. AND HUXLEY, A. F. A quantitative description of membrane current and its application to conduction and excitation in nerve. *J. Physiol. Lond.* 117: 500–544, 1952.

JENKINSON, D. H. The nature of the antagonism between calcium and magnesium ions at the neuromuscular junction. *J. Physiol. Lond.* 138: 434–444, 1957.

KAMIYA, H. AND ZUCKER, R. S. Residual Ca^{2+} and short-term synaptic plasticity. *Nature Lond.* 371: 603–606, 1994.

KATZ, B. AND MILEDI, R. The role of calcium in neuromuscular facilitation. *J. Physiol. Lond.* 195: 481–492, 1968.

LANDÒ, L. AND ZUCKER, R. S. Ca^{2+} cooperativity in neurosecretion measured using photolabile Ca^{2+} chelators. *J. Neurophysiol.* 72: 825–830, 1994.

LIU, Y. AND STANLEY, E. F. Calcium binding sites of the transmitter release mechanism: clues from short-term facilitation. *J. Physiol. Paris* 89: 163–166, 1995.

LLINÁS, R., STEINBERG, I. Z., AND WALTON, K. Presynaptic calcium currents in squid giant synapse. *Biophys. J.* 33: 289–322, 1981a.

LLINÁS, R., STEINBERG, I. Z., AND WALTON, K. Relationship between presynaptic calcium current and postsynaptic potential in squid giant synapse. *Biophys. J.* 33: 323–352, 1981b.

LLINÁS, R., SUGIMORI, M., AND SILVER, R. B. Microdomains of high calcium concentration in a presynaptic terminal. *Science Wash. DC* 256: 677–679, 1992.

LLINÁS, R., SUGIMORI, M., AND SIMON, S. M. Transmission by presynaptic spike-like depolarization in the squid giant synapse. *Proc. Natl. Acad. Sci. USA* 79: 2415–2419, 1982.

MAGLEBY, K. Short-term changes in synaptic efficacy. In: *Synaptic Func-*

tion, edited by G. M. Edelman, L. E. Gall, W. Maxwell, and W. M. Cowan. New York: Wiley, 1987, p. 21–56.

MOLGÓ, J. AND THESLEFF, S. Electronic properties of motor nerve terminals. *Acta Physiol. Scand.* 114: 271–275, 1982.

PARNAS, H., DUDEL, J., AND PARNAS, I. Neurotransmitter release and its facilitation in the crayfish. VII. Another voltage dependent process besides Ca entry controls the time course of phasic release. *Pfluegers Arch.* 406: 121–130, 1986a.

PARNAS, H., HOVAV, G., AND PARNAS, I. Effect of Ca^{2+} diffusion on the time course of neurotransmitter release. *Biophys. J.* 55: 859–874, 1989.

PARNAS, H. AND SEGEL, L. A. Exhaustion of calcium does not terminate evoked neurotransmitter release. *J. Theor. Biol.* 107: 345–365, 1984.

PARNAS, I., PARNAS, H., AND DUDEL, J. Neurotransmitter release and its facilitation in crayfish. VIII. Modulation of release by hyperpolarizing pulses. *Pfluegers Arch.* 406: 131–137, 1986b.

RAHAMIMOFF, R. A dual effect of calcium ions on neuromuscular facilitation. *J. Physiol. Lond.* 195: 471–480, 1968.

RAHAMIMOFF, R. AND YAARI, Y. Delayed release of transmitter at the frog neuromuscular junction. *J. Physiol. Lond.* 228: 241–257, 1973.

REGEHR, W. G., DELANEY, K. R., AND TANK, D. W. The role of presynaptic calcium in short-term enhancement at the hippocampal mossy fiber synapse. *J. Neurosci.* 14: 523–537, 1994.

SHERMAN, A., KEIZER, J., AND RINZEL, J. Domain model for Ca^{2+} -inactivation of Ca^{2+} channels at low channel density. *Biophys. J.* 58: 985–995, 1990.

SIMON, S. AND LLINÁS, R. Compartmentalization of the submembrane calcium activity during calcium influx and its significance in transmitter release. *Biophys. J.* 48: 485–498, 1985.

STANLEY, E. F. Decline in calcium cooperativity as the basis of facilitation at the squid giant synapse. *J. Neurosci.* 6: 782–789, 1986.

STANLEY, E. F. Single calcium channels and acetylcholine release at a presynaptic nerve terminal. *Neuron* 11: 1007–1011, 1993.

STANLEY, E. F., BERTRAM, R., AND SHERMAN, A. The single domain/bound calcium hypothesis of transmitter release and facilitation. *Soc. Neurosci. Abstr.* 21: 24, 1995.

STANLEY, E. F. AND GOPING, G. Characterization of a calcium current in a vertebrate cholinergic presynaptic nerve terminal. *J. Neurosci.* 11: 985–993, 1991.

WINSLOW, J. L., DUFFY, S. N., AND CHARLTON, M. P. Homosynaptic facilitation of transmitter release in crayfish is not affected by mobile calcium chelators: implications for the residual ionized calcium hypothesis from electrophysiological and computational analyses. *J. Neurophysiol.* 72: 1769–1793, 1994.

YAMADA, W. M. AND ZUCKER, R. S. Time course of transmitter release calculated from simulations of a calcium diffusion model. *Biophys. J.* 61: 671–682, 1992.

YOSHIKAMI, D., BAGABOLDO, Z., AND OLIVERA, B. M. The inhibitory effects of omega-conotoxins on Ca channels and synapses. *Ann. NY Acad. Sci.* 560: 230–248, 1989.

YOUNKIN, S. G. An analysis of the role of calcium in facilitation at the frog neuromuscular junction. *J. Physiol. Lond.* 237: 1–14, 1974.

ZENGEL, J. E. AND MAGLEBY, K. L. Changes in miniature endplate potential frequency during repetitive nerve stimulation in the presence of Ca^{2+}, Ba^{2+}, and Sr^{2+} at the frog neuromuscular junction. *J. Gen. Physiol.* 77: 503–529, 1981.

ZUCKER, R. S. AND FOGELSON, A. L. Relationship between transmitter release and presynaptic calcium influx when calcium enters through discrete channels. *Proc. Natl. Acad. Sci. USA* 83: 3032–3036, 1986.